Nonadiabatic effects in photoelectron spectra of HCl and DCl. I. Experiment

F. Burmeister,[1,*] S. L. Sorensen,[2] O. Björneholm,[1] A. Naves de Brito,[3] R. F. Fink,[1] R. Feifel,[1] I. Hjelte,[1] K. Wiesner,[1] A. Giertz,[1] M. Bässler,[2] C. Miron,[1] H. Wang,[2] M. N. Piancastelli,[4] L. Karlsson,[1] and S. Svensson[1]

[1]*Department of Physics, Uppsala University, Box 530, S-751 21 Uppsala, Sweden*

[2]*Department of Synchrotron Radiation Research, Institute of Physics, University of Lund, Box 118, S-221 00 Lund, Sweden*

[3]*Institute of Physics, University of Brasilia, 70910-900 Brasilia DF, Brazil*

[4]*Department of Chemical Sciences and Technologies, University "Tor Vergata," I-00133 Rome, Italy*

(Received 3 July 2001; published 12 December 2001)

The HCl inner-valence photoelectron band at 26 eV binding energy has been recorded at high resolution. Discrete peaks arising from at least two separate vibrational progressions are superimposed on the broad continuum. Fano profiles are visible in one of the progressions. This indicates interference between superimposed electronic states, where weak avoided crossing allows two adiabatic states to couple. In the isotopic DCl molecular spectrum, the discrete lines are less pronounced, due to slower dissociation and therefore less coupling between the continuum and the bound state.

DOI: 10.1103/PhysRevA.65.012704 PACS number(s): 33.80.Eh, 33.70.Ca, 34.50.Gb

I. INTRODUCTION

Interference is a phenomenon arising from the superposition of two wave functions at the same final state. Spatial coherence is required, thus the spatial source extension must be small compared to the wavelength. Temporal coherence is also required in order to allow an interference pattern to be observed. The archetypal example of interference in atomic and molecular physics is the interference between a discrete autoionizing electronic state and a continuum seen in absorption spectra, as described by Fano in 1961 [1]. Fano profiles are found not only in absorption, but are also seen in the electronic decay spectra of, for example, rare-gas core-excited states [2]. Lifetime-vibrational interference, i.e., interference between discrete states, are well documented in core-excited systems in x-ray and Auger emission spectra [3]. A third case, quantum interference between continuum states in core-excited HCl and DCl has recently been reported [4].

Predissociation is an indirect bond-breaking process, which occurs when a molecule is excited to a state embedded in a weakly coupled continuum. Interference between direct and indirect photodissociation of the FNO molecule is a case, which has raised a great deal of interest [5,6]. The wave packet describing the predissociation of FNO bifurcates into two parts, one part leaving the inner region potential energy surface very rapidly while a second part remains temporarily trapped. The direct dissociative part gives rise to a broad, unstructured background in the absorption spectrum, while the ''resonant'' contribution results in the relatively narrow vibrational structure from the N-O stretching progression excited within the quasibound complex. A related interference phenomenon is presented in this paper for photoionization of HCl and the deuterated equivalent DCl. In the photoelectron spectrum, the broad direct dissociative channel is superimposed on the narrow vibrational progression from the resonant contribution of the predissociative state. The relative intensities and phases of these two channels are influenced primarily by the dynamics of the predissociation process.

One way to investigate the dynamics of molecular systems explicitly, is with laser pump-and-probe techniques [7], as, e.g., demonstrated in the case of NaI [8]. The molecular system is pumped to a predissociative state weakly coupled to a continuum. The probability for the system to be in one of the states was probed for different time intervals after the pump pulse. It was found that the continuum state increased in intensity while the predissociative state decreased according to the lifetime of the predissociative state.

HCl is well suited for detailed investigations of dynamical molecular processes. The electronic states have been extensively studied, and many dissociative states appearing in the inner valence region of the photoelectron spectrum are well documented in the literature [9]. The molecule is theoretically tractable even with respect to strong many-electron effects in the inner valence regime, and the interpretation of the experimental spectrum is facilitated by comparatively sparse photoelectron bands, which reduces the overlap of bands in the spectrum. An additional advantage is the presence of only one single vibrational mode of relatively high energy. The identical electronic structure but different reduced masses for HCl and DCl can be exploited spectroscopically in several ways. Hitherto mostly trivial differences between isotopic spectra have been reported in photoelectron spectroscopy, e.g., energy differences in the vibrations for bound states. Deuteration has been used to illuminate the intricate details of dynamics in small molecular systems [10–13].

The ground state configuration of the valence electronic states of HCl is $(4\sigma)^2(5\sigma)^2(2\pi)^4$. The two outermost bands corresponding to ionization of the 2π and 5σ orbitals are easily discernible, whereas the inner-valence region is more complex due to the strong influence of multielectron processes [11,14]. A 2π vacancy leads to spin-orbit split $^2\Pi$ ionic states, whereas 5σ and 4σ vacancies lead to states of $^2\Sigma^+$ symmetry. The inclusion of two-hole–one-particle (2h1p) configurations give additional states, some of which

*Corresponding author. FAX:+46-18 471 3524. Email address: florian.burmeister@fysik.uu.se

have the right symmetry to interact with the single-hole states. Since these many-electron states thus acquire some single hole character, they become observable in photoelectron spectra. The present study focuses on the band at 26 eV binding energy, which is primarily related to the 4σ single-hole state, and additional states appearing in the same energy range.

Assignments of the different bands have been made using Green's function calculations, and an *ab initio* MO CI method [15,9]. More recently, detailed spectra of HCl and DCl in the inner-valence region have been obtained using threshold photoelectron spectroscopy [16,17], and photoelectron spectroscopy [18]. The resolution was sufficient to resolve vibrational structure in several bands. Rotationally resolved PES has been performed on the outer-valence region in HCl, where the bound A state was shown to be weakly coupled to a continuum [19].

According to the Born-Oppenheimer approximation, the nuclear motion of the molecule may be neglected in calculations of the electronic structure and analysis of electron spectra, since the velocity of electrons is much higher than that of the nuclei. Normally, this is a good approximation but there are cases where it does not hold. Second-order perturbation theory dictates that two electronic states with identical symmetry cannot be degenerate at any internuclear distance. They tend to repel each other, and the potential curves associated with these electronic states will not intersect. This is usually referred to as the ''avoided-crossing rule.'' The state of the system will follow the adiabatic potential from one electronic configuration to the other, that is, it always follows the lowest potential curve that exists in that symmetry. But since this framework is based upon an approximation there will be phenomena that cannot be explained using this model. A nonavoided crossing behavior has been reported in photoelectron spectra of O_2 [20]. In this paper, we will present the nonavoided crossing behavior in photoelectron spectroscopy, depending on the different dissociation times for HCl and DCl. A similar effect has been discussed in connection with H^- and D^- production by electron impact [21,22]. The observed differences can be attributed to limitations of the Born-Oppenheimer approximation and the adiabatic framework. A time-dependent picture of the photoionized system including the nuclear dynamics provides a framework for qualitative understanding [23,24].

II. EXPERIMENT

The high-resolution spectra presented in this paper are measured at the state-of-the-art undulator beam line I 411 [25] connected to the third-generation electron storage ring MAX II, at the MAX laboratory in Lund, Sweden. The photon energy used was $h\nu = 64$ eV. The monochromator resolution was set to 10 meV FWHM, and the electron spectrometer resolution was 25 meV FWHM for all spectra. The main axis of the spectrometer lens was set at the magic angle (54.7°) with respect to the plane of polarization of the undulator radiation. HCl gas was obtained commercially from Air Liquide with a purity of $>99.99\%$ and DCl gas of comparable purity was produced in the chemistry laboratory at MAX by reacting D_2SO_4 with NaCl. The purity of both gases was carefully checked by on-line valence photoelectron spectroscopy during measurements.

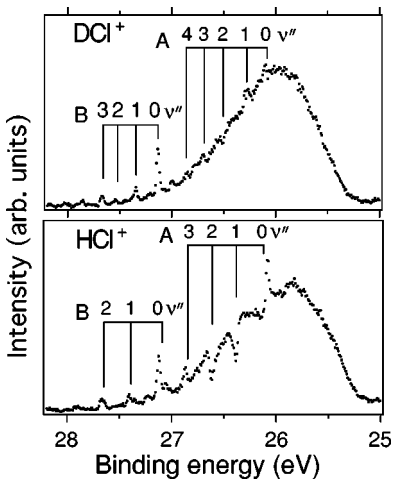

FIG. 1. The ''4σ'' band, with continuum state CS between 25.4 and 27.5 eV, and vibrational progressions A and B for HCl and DCl. The interference between the continuum and the vibrational progression A is clear to see for HCl, but almost disappears for DCl. The difference in vibrational progression intensities is due to the different reduced masses and dissociation velocities.

III. RESULTS

In Fig. 1 the inner-valence band denoted ''4σ'' is presented in detail for the HCl and DCl molecules. The broad profile of the band is due to the steep behavior of the potential energy curve, in the Franck-Condon region. In this band, at least two vibrational progressions denoted A and B are visible in Fig. 1, reflecting the existence of bound states in the region of the continuum state. Vibrational progression B consists of peaks that lie on the tail of the band, corresponding to the continuum state. Vibrational progression A, on the other hand, exhibits a peculiar interference pattern in the HCl spectrum. The $\nu''=0$ peak has a shoulder with a slight dip on the high binding energy side. For the $\nu''=1$ and $\nu''=2$ peaks the distortion of the peak profile is more conspicuous, these ''peaks'' appear essentially as dips, i.e., window resonances. For $\nu''=3$ the peak resembles a symmetric peak on top of the continuum state. For DCl, vibrational progression B shows a behavior similar to the HCl case, but with approximately a factor $1/\sqrt{2}$ smaller energy difference between the vibrational lines, as expected for the difference in reduced mass. In sharp contrast, vibrational progression A almost disappears for DCl. As will be shown, the comparison between the spectra for HCl and DCl strongly indicates that the distortion of the peaks in the vibrational progression A in HCl arises from an interference between the bound and repulsive continuum states. In Fig. 1, hints of further vibrational progressions in the region of interest can be seen. There are peaks appearing around vibrational progression B, which are not being discussed here. By improving experimental resolution, further intriguing details could be revealed.

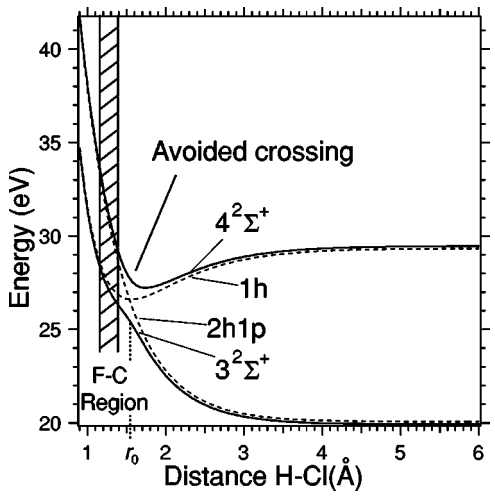

FIG. 2. Potential curves for the electronic states of interest in the inner-valence region in HCl. The adiabatic and diabatic states with assignments are shown as solid and dashed lines, respectively. The Franck-Condon region between 1.16 and 1.39 Å is shown. The avoided crossing influences the adiabatic states around $r_0 = 1.54$ Å.

IV. DISCUSSION

In Fig. 2 two of the potential curves in the inner-valence region of HCl are shown as solid lines with assignments taken from [9]. They are associated with the $3\,^2\Sigma^+$ and $4\,^2\Sigma^+$ ionic states. For short H-Cl distances, the $3\,^2\Sigma^+$ is dominated by the one hole (1h) configuration $(4\sigma)^1(5\sigma)^2(2\pi)^4(6\sigma)^0$ and therefore, a large photoionization cross section is expected for this state. At larger bond distances, however, this state is dominated by the two-hole one-particle, 2h1p, configuration $(4\sigma)^2(5\sigma)^0(2\pi)^4(6\sigma)^1$ with an appreciable mixing of the 2h1p configuration $(4\sigma)^2(5\sigma)^2(2\pi)^2(6\sigma)^1$. For $4\,^2\Sigma^+$ the configuration dominance is reversed compared to $3\,^2\Sigma^+$. The solid lines in Fig. 2 refer to adiabatic potential curves from [9]. The dashed lines are the related diabatic potential curves corresponding to 1h $(4\sigma)^1(5\sigma)^2(2\pi)^4(6\sigma)^0$ and 2h1p $(4\sigma)^2(5\sigma)^0(2\pi)^4(6\sigma)^1$ configurations. These curves have been obtained in the present study by assuming a Morse potential for the bound diabatic state, and a repulsive exponential function for the unbound state. Furthermore, vibrational progression B is suggested to correspond to $(4\sigma)^2(5\sigma)^2(2\pi)^2(1\delta)^1$, i.e., a 2h1p state with two holes in 2π and one particle in a δ Rydberg orbital [15,17].

The Franck-Condon region between 1.16 and 1.39 Å is shown in Fig. 2. The spectrum expected from a consideration of the Franck-Condon factors for the adiabatic $3\,^2\Sigma^+$ and the diabatic 1h states is a broad band between 25.4 and 27 eV binding energy related to the dissociative $3\,^2\Sigma^+$ state, and a vibrational progression starting around 26 eV related to the bound 1h state. As can be seen in Fig. 1, this matches fairly well the experimental result. Such an assignment including the adiabatic $3\,^2\Sigma^+$ final-state potential as well as the diabatic 1h potential in a discussion invoking the Franck-Condon picture, is due to limitations of the adiabatic framework, as will be discussed more thoroughly below. The kinematics of the process clearly plays a role in the curve-crossing mechanism in conflict with the premises of the Born-Oppenheimer approximation. We therefore discuss the process both in a time-dependent and in a time-independent picture.

In a time-independent framework the interference pattern between vibrational progression A and the continuum state can qualitatively be described as follows. When two wave functions related to different potential curves give the same internal energy, the Franck–Condon projection of the initial state wave function is made onto the sum of the two final state wave functions. The experimentally observed intensities are the square of the modulus of the sum of the amplitudes. This sum contains a term that depends upon the relative phases of the superimposed waves; the interference term. This term may dominate the intensity and even result in a negative, destructive total intensity.

The predissociative nature of the 1h state implies dissociation following $3\,^2\Sigma^+$ as the final state, which is the same as for the direct dissociation path. The kinetic energy of the outgoing electron will be the same independent of whether the direct or predissociative path is followed. The criteria for interference between the channels are hereby fulfilled.

The use of the bound diabatic 1h state in the discussion remains to be clarified. In pump-and-probe experiments, where the evolution of molecular systems with time can be probed explicitly, the probability of ''hopping'' from one adiabatic curve to another has been found to be nonzero in some studied systems [8]. The crossing between adiabatic curves for a system is equivalent to remaining on the same diabatic curve. In our nontime-resolved experiment, the probability amplitudes for adiabatic and diabatic paths to the same final state are manifested as interference.

In the adiabatic description of the molecule potential surfaces never cross, but the electronic structure changes with the internuclear distance. For this to be valid the internuclear distance r is supposed to increase infinitely slowly (Born-Oppenheimer approximation), so that the electrons, which are very mobile, can follow ''adiabatically'' the motion of the nuclei and change configuration with distance. In the present case, this means a change from 2h1p character to 1h character for the upper $4\,^2\Sigma^+$ state, and from 1h to 2h1p character for the lower $3\,^2\Sigma^+$ state with increasing r, as discussed in connection to Fig. 2. The molecule will then remain in one adiabatic state with zero probability for crossing the other one. But if r changes with a finite rate, the electrons cannot completely follow adiabatically the motion of the nuclei and change configuration with distance. There will then be a finite probability that the molecule will change from one adiabatic curve to another as it passes $r=r_0$, so that its final electronic state can be represented by a linear combination of adiabatic states. There are the following two typical cases representing different physical processes: the case of the same sign of slopes of diabatic potentials (Landau-Zener case) [23,26] and the case of the opposite sign (nonadiabatic tunneling case), which is the case for our discussion. Recent theoretical treatment of both cases can be found in the literature [27–31] and references therein. Treating the linear combination time dependently, one can define the Massey parameter $[W_i(r)-W_j(r)]\delta R/\hbar v$, where $[W_i-W_j]$ is the

adiabatic energy difference at r_0, δR is the characteristic length, and v is the velocity of the system [24]. The Massey parameter is a measure of the validity of the purely adiabatic framework, where a large value ($\gg 1$) justifies an adiabatic description of the system. The difference between the two spectra in Fig. 1 can be explained as the difference between the reduced mass which implies different velocity v and Massey parameter. For the HCl case, v is too large for an adiabatic description of the system, and a linear combination of the two diabatic states in Fig. 2 is required. Since one of the two diabatic potential curves is bound, we observe the vibrational progression A. For DCl v is lower, the Massey parameter is larger, and the adiabatic description is more appropriate. The vibrational progression A almost vanishes. However, the remaining part of the system in the bound state couples less to the continuum, and the lifetime increases. The vibrational progression hereby inhibits a narrower energetic bandwidth. The resolution in our experimental setup is too low for resolving the vibrations properly for DCl. Furthermore, the Franck-Condon overlap between the ground state and the diabatic 1h state for DCl is smaller, due to smaller extension of wave functions in the ground state for the deuterated system. This velocity-dependent interference is seen for the first time in photoelectron spectroscopy. In a forthcoming publication, a theoretical time-dependent calculation with respect to the HCl and DCl systems will be presented, which will support our purely qualitative interpretation [32].

V. CONCLUSIONS

In conclusion, the "4σ" inner-valence band in HCl has been studied using photoelectron spectroscopy. Interference between a dissociative state and a predissociative diabatic state has been observed. Two adiabatic states interfere, and weak avoided crossing between the states allow curve crossing in HCl. In the isotope system DCl, coupling between state is reduced due to slower dissociation velocity, and the vibrational progression is less pronounced.

ACKNOWLEDGMENTS

The support of the MAX-lab staff is gratefully acknowledged. We thank B. Nelander for providing the sample. Support from the Swedish Natural Science Research Council (NFR), the Swedish Foundation for Strategic Research (SSF), the Swedish Research Council for the Engineering Sciences (TFR), and the Swedish Foundation for International Cooperation in Research and Higher Education (STINT) is gratefully acknowledged. A.N.B. thanks the National Council for Scientific and Technological Development (CNPq-Brazil) for financial support. (C.M.) thanks the Knut and Alice Wallenberg Foundation and R.F. acknowledges the support of the Wennergren Foundation.

[1] U. Fano, Phys. Rev. **124**, 1866 (1961).
[2] R.R.T. Marinho *et al.* (unpublished).
[3] F.K. Gel'mukhanov and H. Ågren, Phys. Rep. **312**, 87 (1999).
[4] R. Feifel *et al.*, Phys. Rev. Lett. **85**, 3133 (2000).
[5] R. Cotting, J.R. Huber, and C. Engel, J. Chem. Phys. **100**, 1040 (1994).
[6] A.J. Dobbyn, M. von Dirke, R. Schinke, and R. Fink, J. Chem. Phys. **102**, 7070 (1995).
[7] J. Manz and L. Wöste, *Femtosecond Chemistry* (Wiley, London, 1994), p. 74.
[8] L.R. Khundkar and A.H. Zewail, Annu. Rev. Phys. Chem. **41**, 15 (1990).
[9] M. Hiyama and S. Iwata, Chem. Phys. Lett. **210**, 187 (1993).
[10] O. Björneholm *et al.*, Phys. Rev. Lett. **79**, 3150 (1997).
[11] S. Svensson *et al.*, J. Chem. Phys. **89**, 7192 (1988).
[12] E. Kukk *et al.*, Phys. Rev. Lett. **76**, 3100 (1996).
[13] A.N. de Brito *et al.*, Chem. Phys. Lett. **309**, 377 (1999).
[14] M.Y. Adam, Chem. Phys. Lett. **128**, 280 (1986).
[15] W. von Niessen *et al.*, J. Chem. Phys. **92**, 4331 (1990).
[16] A.J. Yencha *et al.*, J. Electron Spectrosc. Relat. Phenom. **73**, 217 (1995).
[17] A.J. Yencha *et al.*, J. Electron Spectrosc. Relat. Phenom. **238**, 109 (1998).
[18] A.A. Wills *et al.*, J. Phys. B **26**, 2601 (1993).
[19] D. Edvardsson *et al.*, J. Electron Spectrosc. Relat. Phenom. **73**, 105 (1995).
[20] P. Baltzer *et al.*, Phys. Rev. A **45**, 4374 (1992).
[21] G.J. Schulz, Phys. Rev. **113**, 816 (1959).
[22] Y.N. Demkov, Phys. Lett. **15**, 235 (1965).
[23] H. Eyring, J.E. Walter, and G.E. Kimball, *Quantum Chemistry* (Wiley, New York, 1944), p. 326.
[24] M.S. Child, *Molecular Collision Theory* (Academic, London, 1974), p. 88.
[25] M. Bässler *et al.*, Nucl. Instrum. Methods (to be published).
[26] E. Majorana, Nuovo Cimento **9**, 43 (1932).
[27] C. Zhu and H. Nakamura, J. Chem. Phys. **101**, 4855 (1994).
[28] C. Zhu and H. Nakamura, J. Chem. Phys. **101**, 10 630 (1994).
[29] C. Zhu and H. Nakamura, J. Chem. Phys. **102**, 7448 (1995).
[30] V.I. Osherov and H. Nakamura, J. Chem. Phys. **105**, 2770 (1996).
[31] V.N. Ostrovsky and H. Nakamura, J. Phys. A **30**, 6939 (1997).
[32] L.M. Andersson, F. Burmeister, H. Karlsson, and O. Goscinski, Phys. Rev. A **65**, 012705 (2002).